

Why Do AGN Lighthouses Switch Off?

Ramesh Narayan

Harvard-Smithsonian Center for Astrophysics, 60 Garden Street, Cambridge, MA
02138, U.S.A.

Abstract. Nearby galactic nuclei are observed to be very much dimmer than active galactic nuclei in distant galaxies. The Chandra X-ray Observatory has provided a definitive explanation for why this is so. With its excellent angular resolution, Chandra has imaged hot X-ray-emitting gas close to the gravitational capture radius of a handful of supermassive black holes, including Sgr A* in the nucleus of our own Galaxy. These observations provide direct and reliable estimates of the Bondi mass accretion rate \dot{M}_{Bondi} in these nuclei. It is found that \dot{M}_{Bondi} is significantly below the Eddington mass accretion rate, but this alone does not explain the dimness of the accretion flows. In all the systems observed so far, the accretion luminosity $L_{acc} \ll 0.1\dot{M}_{Bondi}c^2$, which means that the accretion must occur via a radiatively inefficient mode. This conclusion, which was strongly suspected for many years, is now inescapable. Furthermore, if the accretion in these nuclei occurs via either a Bondi flow or an advection-dominated accretion flow, the accreting plasma must be two-temperature at small radii, and the central mass must have an event horizon. Convection, winds and jets may play a role, but observations do not yet permit definite conclusions.

1 Introduction

At high redshift, many galactic nuclei are extremely bright, with luminosities in excess of 10^{45} erg s⁻¹. These active galactic nuclei (AGN) are believed to be powered by accretion of gas onto supermassive black holes (SMBHs) at nearly the Eddington rate [1]. The accretion very likely occurs via a Shakura-Sunyaev thin disk [2],[3],[4],[5]. The Big Blue Bump, which is present in the spectra of all bright AGN, is identified with blackbody emission from the optically thick disk [6], while the X-ray emission (roughly 10% of the luminosity) is thought to be produced by an optically thin corona above the disk [7],[8]. In addition, most AGN have substantial infrared emission, usually the result of dust reprocessing at a relatively large distance from the SMBH. Some AGN also have significant radio emission from relativistic jets.

Most galactic nuclei at low redshift are very different. These nearby nuclei are much less active — sometimes not active at all. The nuclear source in our own Galaxy, Sagittarius A*, is a particularly good example of a dim galactic nucleus. Studies of AGN demographics suggest that a significant fraction of (perhaps all?) SMBHs must have gone through an AGN “lighthouse” phase at some early stage in their lives. Why and how did these early lighthouses switch off to become the dormant nuclei we see today?

The reduced activity in nearby galactic nuclei is certainly not because of a lack of SMBHs. Recent observations have provided ample evidence that virtually

every galaxy in our local neighborhood has a SMBH [9]. The lack of activity must therefore be the result of reduced gas supply. While this is certainly part of the answer, we shall see that it is not the whole story. A second, equally important, reason is that the very mode of accretion is different in dim nuclei: the accretion occurs via a radiatively inefficient mode, such that even what little gas reaches the SMBH produces much less radiated energy per unit accreted mass than in bright AGN. We review below the evidence for this conclusion. Our primary emphasis is on the nearest and best-studied dim SMBH, Sgr A*, but we also discuss briefly other dim nuclei. The focus is on the observations and on what we can or cannot tell with confidence from the presently available data.

2 Observations of Sgr A*

2.1 Spectrum

Figure 1 summarizes the available data on the spectrum of Sgr A* [10],[11],[12],[13],[14]. Until recently, Sgr A* had been firmly detected only in the radio and millimeter bands, where the source has a hard rising spectrum. There are useful upper limits in the submillimeter and infrared bands which indicate that the emission peaks in the submillimeter/far infrared region of the spectrum, with a luminosity of about 10^{36} erg s $^{-1}$. Sgr A* may have been detected during one observation at $2.2 \mu\text{m}$ [15], with a luminosity of 10^{35} erg s $^{-1}$, but the detection was not confirmed in other observations. If the source is variable, the lone detection may

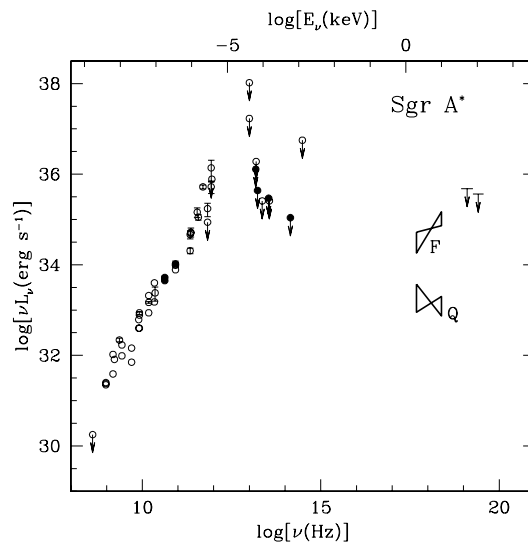


Fig. 1. Spectral data on Sgr A*. Shown is νL_ν , the luminosity per logarithmic interval of frequency ν , versus ν (lower scale) or photon energy $E_\nu = h\nu$ (upper scale).

represent its brightest state. The data point is shown as an upper limit in Fig. 1. In the optical, UV and soft X-ray bands, the source is strongly extinguished (visual extinction $A_V \approx 30$ magnitudes [20]) and there are no direct constraints on the spectrum. Nevertheless, it is generally agreed that the emission in these hidden bands is unlikely to exceed that in the submillimeter peak.

Over the years, Sgr A* has been observed many times in X-rays [16],[18],[17],[19]. However, because the source is very weak and the field is highly crowded, there was no unambiguous detection until the recent observations of Baganoff et al. [13],[14] with the Chandra X-ray Observatory. The exquisite angular resolution of Chandra allowed Sgr A* to be isolated within the crowded field and its flux and spectrum to be measured. Out of a total of 76 ks of observations, extending over two epochs, the source was in a quiescent state (marked Q in Fig. 1) for nearly 70 ks, with a flux of 2.2×10^{33} ergs $^{-1}$ and a relatively soft spectrum (photon index $\Gamma \sim 1.6 - 2.8$ [14]). For a brief period of several ks during the second epoch of observation, the source went into a flare state (F in Fig. 1), during which the flux went up by a factor of a few tens and the spectrum became quite hard ($\Gamma \sim 0.7 - 1.8$). Integrated over time, the emission in the flare was small compared to the quiescent emission. We therefore take the quiescent data as representative of the average properties of the source. We discuss the flare briefly in §5.3.

The mass of the SMBH at the center of our Galaxy has been measured to be $2.6 \times 10^6 M_\odot$ [21],[22],[23],[24], which means that the Eddington luminosity of Sgr A* is $L_{Edd} = 3 \times 10^{44}$ ergs $^{-1}$. On the scale of L_{Edd} , the peak emission in the submillimeter is $L_{submm} \sim 10^{-8.5} L_{Edd}$. The luminosity in the infrared is even less, $L_{IR} < 10^{-9.5} L_{Edd}$, and the quiescent X-ray luminosity is a pitiful $L_X \sim 10^{-11} L_{Edd}$. Thus, Sgr A* is an extremely dim galactic nucleus. Indeed, it is the dimmest nucleus for which we have useful data, which explains why this source plays such a central role in all discussions of dim galactic nuclei.

2.2 Bondi Accretion Rate

In a famous paper, Bondi [25] discussed the problem of spherical hydrodynamical accretion onto a black hole (BH) of mass M immersed in a uniform medium of density ρ_0 and sound speed $c_{s,0}$. He showed that the sphere of influence of the BH extends out to the gravitational capture radius $R_c = GM/c_{s,0}^2$. Gas external to R_c is only mildly perturbed by the BH, whereas any gas that falls within R_c is gravitationally captured by the BH and free-falls down to the center. The radial velocity in the free-fall zone is

$$v_R \sim (2GM/R)^{1/2} \sim c_{s,0}(R/R_c)^{-1/2}, \quad (1)$$

and so the mass accretion rate onto the BH is approximately (see Bondi's original article or [26] for exact results)

$$\dot{M}_{Bondi} \sim 4\pi R_c^2 \rho_0 c_{s,0}. \quad (2)$$

Bondi’s model applies strictly to a uniform infinitely extended medium. However, even if the external medium is not truly uniform, the above formula for \dot{M}_{Bondi} is still valid, provided we use for ρ_0 the density near the capture radius R_c .

Until recently, the Bondi accretion rate in Sgr A* could be estimated only indirectly, by estimating what fraction of the winds ejected by surrounding stars is captured by the SMBH (see [27],[28]). The estimate had large uncertainties. Chandra has changed the situation dramatically by directly imaging hot X-ray-emitting thermal gas in the vicinity of the capture radius of the SMBH [13]. The observations show that there is extended ~ 1 keV gas with a number density $n_0 \sim 30 \text{ cm}^{-3}$ over an area in the sky of about 10 arcsec around Sgr A*. In addition, there is ~ 2 keV gas with $n_0 \sim 100 \text{ cm}^{-3}$ spread over about an arcsec around the source (and clearly resolved by Chandra [13]). The capture radius of Sgr A* for keV gas is about 1 arcsec (for a BH mass of $2.6 \times 10^6 M_\odot$ and a distance of 8.5 kpc), so the 2 keV emission presumably comes from gas that has just been captured by the BH and been mildly heated by compression. Thus, Chandra provides a direct measurement of the properties of the gas (n_0 and $c_{s,0}$) right at the capture radius. Using this, one can obtain a reliable estimate of the Bondi accretion rate [13]:

$$\dot{M}_{Bondi} \sim (0.3 - 1) \times 10^{-5} M_\odot \text{yr}^{-1} \sim 3 \times 10^{20} \text{ g s}^{-1} \sim 10^{-4} \dot{M}_{Edd}, \quad (3)$$

where we have formally assumed a radiative efficiency of 10% in the definition of the Eddington accretion rate, i.e. $\dot{M}_{Edd} \equiv L_{Edd}/0.1c^2$.

3 There is No Thin Disk in Sgr A*

Could Sgr A* have a Shakura-Sunyaev thin disk? In the most straightforward version of this model, mass would flow onto the disk at the Bondi rate \dot{M}_{Bondi} estimated in (3) and would flow steadily through the disk onto the SMBH. The model would predict a luminosity $L_{disk} \sim 0.1 \dot{M}_{Bondi} c^2 \sim 10^{40.5} \text{ erg s}^{-1}$, with the bulk of the emission appearing in the near infrared and optical bands. Figure 2 shows model spectra corresponding to a thin disk with three choices of \dot{M} : $(10^{-6}, 10^{-7}, 10^{-8}) \times \dot{M}_{Edd}$. Even models with such low accretion rates, which are far lower than \dot{M}_{Bondi} , are ruled out by the infrared limits.

One way of trying to save the thin disk model is to assume that gas flows in at the Bondi rate at R_c , but then condenses onto a cold “dead” disk where it sits without accreting onto the BH. This would require the disk to be in a very quiet state with an extremely low viscosity. This is not unreasonable — for instance, cataclysmic variables and soft X-ray transient binaries have quiescent states in which the gas accretes onto the central mass at a much lower rate than the rate at which gas is fed on the outside by mass transfer from the companion star. In the case of Sgr A*, however, such a model runs into difficulties because the inflowing gas would produce a fair amount of luminosity in the infrared, and possibly also X-rays, as it crashes onto the thin disk and loses its thermal and kinetic energy [29]. For example, cataclysmic variables and X-ray transients in quiescence have optical and UV emission from the “hot spot” where the incoming gas stream hits

the disk, even though the disk itself may be hardly accreting. The lack of any evidence for thermalization radiation from the inflowing gas rules out the thin disk model quite strongly in Sgr A*. In the opinion of this author, any variant of the model that succeeds in getting round this constraint is likely to be very contrived. We will therefore take it as given that there is no thin disk in Sgr A*.

As an aside, we note that the above argument does not apply if the accretion occurs via an advection-dominated accretion flow (see §§5.1,5.2) instead of a thin disk (despite claims to the contrary [12]). The reason is that in the case of an advective flow, there is no free-falling Bondi-like zone. At the capture radius the gas directly makes a transition to a subsonic rotating accretion flow, and there is no supersonic zone or shock. (In addition, even if there were a shock it is not clear that the hot gas would radiate very much, as it is advection-dominated.)

Returning to the discussion on thin disk models, the essence of the argument against the presence of a thin disk in Sgr A* is the fact that the accretion luminosity L_{acc} is very low,

$$L_{acc} \ll 0.1 \dot{M}_{Bondi} c^2, \quad (4)$$

whereas a thin disk, being radiatively efficient, will normally have $L_{acc} \sim 0.1 \dot{M}_{Bondi} c^2$. If Sgr A* does not have a thin disk, then what kind of a flow does it have? Whatever the flow is, the data tell us that it has to be radiatively highly inefficient. Radiatively inefficient gas will be hot, because the energy has nowhere to go except into thermal energy. The gas will also be quasi-spherical rather than thin. We now turn to a consideration of models with these properties.

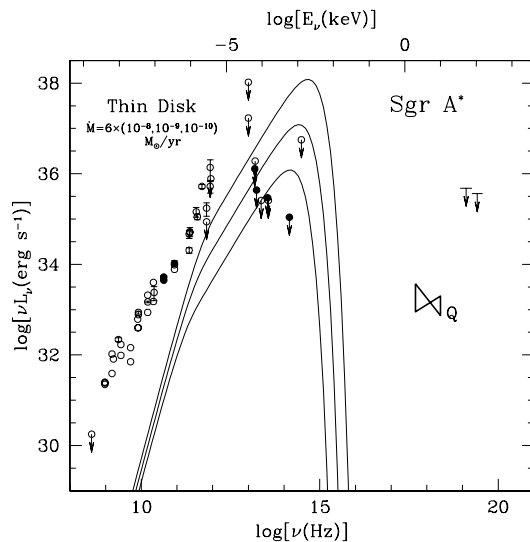


Fig. 2. Spectra corresponding to thin disk models of Sgr A* with three choices of \dot{M} . All three models shown have $\dot{M} \ll \dot{M}_{Bondi}$. Yet, all three models are too bright to fit the data.

4 Bondi Model

4.1 Spherical Accretion

The most famous example of a radiatively inefficient accretion flow is Bondi spherical accretion [25]. The radial velocity of the accreting gas and the mass accretion rate in this model are given by (1) and (2) above. From these, the density profile is easily obtained: $\rho \sim \rho_0(R/R_c)^{-3/2}$, where ρ_0 is the density of the external medium.

Bondi originally assumed that the accreting gas is neither heated nor cooled. This assumption is not valid if the gas is magnetized. As Shvartsman [30] first argued, any magnetic field frozen in the gas is amplified as $B \propto R^{-2}$, and so the magnetic energy density grows as R^{-4} . The gas energy density, however, varies only as $R^{-5/2}$, which means that even if the gas starts off with a sub-equipartition strength B , the field quickly grows to equipartition strength at some radius. Inside this radius, the field will reconnect so as to maintain rough equipartition. The reconnection will heat the gas [31], and as a result, the thermal energy will come roughly into equipartition with the magnetic energy. Since there is negligible cooling, the sum of the thermal, magnetic and kinetic energies should equal the potential energy of the gas. It is then easy to show that the temperature of the gas will vary roughly as

$$T \sim 10^{12}(R/R_S)^{-1} \text{ K}, \quad c_s \sim c(R/R_S)^{-1/2}, \quad (5)$$

where $R_S = 7.7 \times 10^{11}(M/2.6 \times 10^6 M_\odot)$ cm is the Schwarzschild radius of the accreting BH.

The heating of the gas leads to convection; we discuss this topic in §7.1.

4.2 Bondi Models of Sgr A*

Given the above profiles of density and temperature, it is straightforward to calculate the spectrum of a Bondi accretion flow. The primary emission mechanisms are synchrotron and bremsstrahlung, plus Comptonization of each. The solid line in Fig. 3 shows the predicted spectrum of Sgr A* if accretion occurs via a Bondi flow. We have normalized the density of the model such that, at $R = R_c$, the density is equal to ρ_0 as measured by Chandra. The model clearly predicts far too much flux all across the spectrum. The reason is the very high temperature of the electrons, especially close to the BH (see eq 5). The hot electrons radiate synchro-Compton emission very efficiently.

A Bondi model for Sgr A* was proposed by Melia [32],[33] many years ago and pursued in detail by his group. This work was the first to propose that a hot accretion flow emitting synchrotron and bremsstrahlung radiation could explain the strange properties of Sgr A*.

The published models of Melia fit the observed spectrum quite well, which is rather surprising considering that we find the Bondi model to overpredict the luminosity by many orders of magnitude (solid line in Fig. 3). More surprising

still, the Melia models used an accretion rate 100 times larger than the one used here in Fig. 3, and yet agreed with the observations. One reason for the large discrepancy is an error (at least in the early work) in the computation of the synchrotron spectrum (see [34]). Another reason could be that Compton-scattering was not included in some of the models. It is also possible that the models did not correctly include heating due to magnetic dissipation. Strong heating is generic to any spherical flow that falls over many decades of radius (§4.1). The heating can be avoided if the magnetic field is extraordinarily weak in the external medium so that the field does not grow to equipartition strength even at the BH horizon, but this is very unlikely. Alternatively, heating would be weak if the field reconnects while it is still well below equipartition, as proposed in some models [35]. But this requires the reconnection to proceed at much faster than the Alfvén speed, which seems unlikely (e.g., [36],[37]).

The electrons in a Bondi model of Sgr A* are too luminous because they are too hot. This suggests a possible fix: make the accreting plasma two-temperature, with the electrons much cooler than the protons. Two-temperature models of spherical flows were developed in detail by Shapiro and co-workers for accretion flows onto neutron stars [38] and BHs [39]. If one assumes that ions and electrons couple only via Coulomb collisions — a not unreasonable assumption — then at the low density of the accretion flow in Sgr A*, the plasma would automatically develop a two-temperature structure.

To illustrate how strong an effect the electron temperature has on the spectrum, we consider an artificial problem in which we modify the electron tempera-

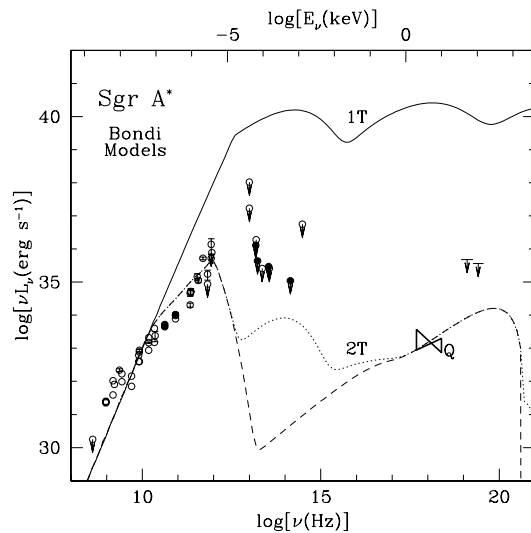


Fig. 3. Spectra of Sgr A* corresponding to Bondi spherical accretion models (see the text for details)

ture profile in the Bondi flow such that it is capped at 10^{10} K. The model predicts the spectrum shown by the dotted line in Fig. 3 (the dashed line is the contribution due to bremsstrahlung and synchrotron alone, without Comptonization). This model is clearly in much better agreement with the observations than the one-temperature model (solid line). We thus conclude that any successful model of Sgr A* is likely to involve a two-temperature plasma.

Before closing this section, we note that the spherical accretion model, while good for developing insight into the properties of hot flows, is unlikely to describe real accretion flows since it ignores the angular momentum of the accreting gas. In almost any accretion flow, the gas is likely to possess sufficient angular momentum that it would hit the centrifugal barrier at some radius R_{cb} before it can fall into the BH. Inside R_{cb} , accretion is possible only if there is some agency to transfer angular momentum outward; we will call this agency “viscosity” though it is probably magnetic stresses [40]. Some authors have proposed models in which they invoke a Bondi flow from the capture radius R_c down to R_{cb} , and they then introduce a thin disk or some other kind of rotating solution from R_{cb} down to the marginally stable orbit (e.g., [33],[41]). The problem with any such model is that there is nowhere for the angular momentum to go. A viscous rotating flow can accrete only if it can get rid of angular momentum to the outside, but angular momentum cannot be transported across supersonic zones such as a Bondi flow [42],[43]. Therefore, if the supersonically infalling gas in a Bondi-like flow is arrested by centrifugal forces, then whatever rotating structure forms at the center must extend out at least to the capture radius in order to be able to transfer angular momentum to the outside. Many models of Sgr A* in the literature fail to satisfy this simple consistency condition. (The ADAF model discussed next does satisfy the condition.)

5 Advection-Dominated Accretion Flow (ADAF) Model

5.1 The ADAF Model

The thin accretion disk is a radiatively efficient model in which all the energy released through viscous dissipation is radiated away. One could describe it as a cooling-dominated accretion flow. An “advection-dominated accretion flow” (ADAF) is one in which most of the heat energy released by viscosity and compression is retained in the gas and advected to the center, and only a very small fraction of the energy is radiated.

Technically, any radiatively inefficient accretion flow, including the Bondi flow, is advection-dominated. However, the term ADAF is conventionally applied only to a particular class of quasi-spherical models that include rotation, viscosity and a two-temperature plasma [44],[45],[46],[47],[48], [49][50]. We will follow this convention here.

The reason ADAFs are advection-dominated is that the accreting gas has a low density (because of the low mass accretion rate) and the thermal structure of the plasma is two-temperature. Because of the low density, very little of the heat

energy in the ions gets transferred to the electrons through Coulomb collisions [39],[48], [51]. Since the ions hardly radiate at all, they retain their thermal energy and advect essentially all of it to the center. The ion temperature thus scales essentially as in (5) and becomes of order 10^{12} K near the BH. The electrons do radiate some of their energy. They also have a different equation of state once they become relativistic (at small radii). For both reasons, they are cooler than the ions, and do not get much hotter than $\text{few} \times 10^{10}$ K near the BH. The lower temperature makes the electrons less efficient radiators than in the one-temperature Bondi model shown in Fig. 3. Indeed, at sufficiently low \dot{M} (as in Sgr A*), the electrons become radiatively quite inefficient, though not as inefficient as the ions, and advect a large part of their energy. In this regime, the overall radiative efficiency of the accretion flow can be very low.

Most ADAF models in the literature assume that the ions and electrons have thermal energy distributions, which is reasonable under many conditions [52]. A few papers have considered the effects of nonthermal particles, e.g., [53],[54],[55].

Because the gas in an ADAF has angular momentum, accretion is driven by viscosity (not just gravity as in the Bondi flow). The radial velocity of the gas then scales roughly as $v_R \sim \alpha(GM/R)^{1/2}$ [46], where α is the usual dimensionless viscosity parameter [2],[5]. The velocity is thus lower than in a Bondi flow by a factor $\sim \alpha$, whose typical value is ~ 0.1 . The lower radial velocity means that, for a given ambient density in the external medium, \dot{M}_{ADAF} in an ADAF is lower than \dot{M}_{Bondi} in a Bondi flow by a factor $\sim \alpha \sim 0.1$.

The ADAF solution is allowed only for relatively low values of \dot{M} , less than a few per cent of the Eddington rate for $\alpha \sim 0.1$ [45],[48],[56] (but see [57]). This makes the solution a natural choice for modeling low-luminosity accretion flows. Unlike other hot accretion flow solutions [39],[58], the ADAF does not suffer from any serious thermal or viscous instability [59],[60],[61],[62].

The reader is referred to the following reviews for more details of the ADAF model and its application to dim accretion sources: [63],[64],[65],[66].

5.2 ADAF Models of Sgr A*

ADAF models of Sgr A* have been described in a number of papers in the literature [67],[68],[11],[69],[54],[55],[70]. These studies have shown that it is possible to explain both the very low luminosity of Sgr A* and its spectrum without invoking an unreasonably low mass accretion rate. The above studies were done before the recent Chandra observations, when there was only a rough estimate of the mass accretion rate. Here we present some new results using the Chandra measurement of the density and temperature of the external medium.

Figure 4 shows spectra corresponding to three ADAF models of Sgr A*. The models assume $\alpha = 0.1$ (the results are not sensitive to the precise value) and take the magnetic pressure in the gas to be a tenth of the total pressure. The density profile is matched to the ambient density of the external medium at the capture radius; more precisely, the models have been adjusted so that the predicted bremsstrahlung emission agrees with the spatially resolved X-ray flux measured by Chandra. Because we have used a boundary condition on the density, these

ADAF models have a lower mass accretion rate, $\dot{M}_{ADAF} \sim 10^{-6} M_{\odot} \text{yr}^{-1}$, than the Bondi models described in §4.2. This is to be expected since the radial velocity in an ADAF is lower by a factor $\sim \alpha$ than in a Bondi flow. Note that, because we allow the ADAF to extend all the way out to the capture radius, there is no Bondi-like segment in the accretion flow. The external gas directly makes a transition to the ADAF. The flow is subsonic all the way down to a sonic radius close to the BH, and there is viscous coupling between the accretion flow and the external medium. This allows angular momentum to be expelled from the system to the outside.

The three models shown in Fig. 4 differ in the value of a parameter δ , which measures the fraction of the viscous energy that goes into the electrons. Early ADAF models assumed that nearly all the viscous heat goes into the ions and that δ is very small, say ~ 0.01 . The solid curve in Fig. 4 shows the spectrum for this choice of δ . The spectrum was calculated by the methods described in [11]. We see that the calculated spectrum is generally consistent with the data, though the X-ray spectrum may be a little too hard [13].

Is it reasonable to assume that electrons receive such a small fraction of the viscous heat energy [71]? Several authors have investigated this question [72],[73],[74],[75],[76]. In brief, while it appears that negligible electron heating is possible under some conditions, under other conditions electrons are expected to receive a good fraction (few tenths) of the energy. The short-dashed curve in Fig. 4 shows the predicted spectrum for a model with $\delta = 0.3$. It is reassuring that this model, which uses a “reasonable” value of δ , is again in pretty good agreement with the data. In fact, the model predicts a somewhat softer X-ray

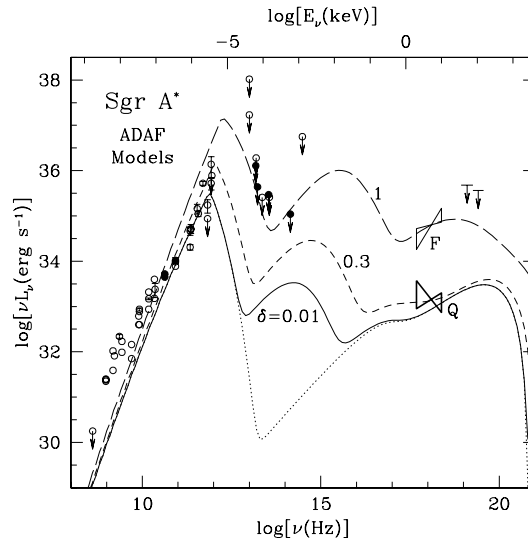


Fig. 4. ADAF models of Sgr A* (see the text for details)

spectrum than the $\delta = 0.01$ model (because part of the emission is now due to Comptonization), which agrees better with the Chandra data.

The dotted line in Fig. 4 corresponds to the contributions from synchrotron and bremsstrahlung emission alone for the $\delta = 0.01$ model. The synchrotron peak on the left nicely fits the radio/mm data, and cuts off where it should in order to satisfy the infrared upper limits. This emission comes from fairly small radii in the flow (few to few tens of R_S). The bremsstrahlung peak on the right explains the quiescent X-ray emission in Sgr A* and is almost entirely from large radii $\sim R_c \sim 10^5 R_S$, which corresponds to an angular scale of order an arcsec. The rest of the emission in the spectrum is from Compton scattering, which fills in the region between the synchrotron and bremsstrahlung peaks. The Compton emission comes primarily from radii inside $100R_S$. It is very reassuring that the model does not produce too much Compton emission in X-rays, since the Compton emission would be spatially unresolved, whereas Chandra has clearly shown that at least 50% of the observed X-ray emission in quiescence is resolved. Overall, we conclude that an ADAF model with $\delta < 0.3$ is consistent with all the presently available data on Sgr A*. Note that, since Chandra has fixed the accretion rate, and since the results are insensitive to α and the details of the magnetic field strength, the model is almost parameter-free. The only parameter that has been adjusted is δ , and even this parameter has a reasonably wide range of allowed values.

As an aside, we note that the argument we made in §3 (second paragraph) against the presence of a “dead” thin disk in Sgr A* does not apply to the ADAF model. Since the ADAF extends all the way out to the capture radius, there is no supersonically infalling region, and therefore there is no shock where the infalling gas may thermalize and radiate the incoming kinetic energy. Another point is that the ADAF model does not require the incoming gas to have a high specific angular momentum. As discussed in §4.2, so long as there is sufficient angular momentum to prevent the gas from falling into the BH directly, a rotating viscous ADAF will grow to the size of the capture radius. Only then can angular momentum be transported out into the ambient medium. For the same reason, the CDAF solution discussed in §7 again has to extend out to the capture radius. In that case, it is not only angular momentum that needs to be transported to the outside, but also a great deal of energy.

Figure 5 shows the profiles of the ion and electron temperatures in the ADAF models discussed above. These profiles have been calculated self-consistently (see [11]), with separate energy equations for the ions and the electrons [77], and assuming that the two species couple only via Coulomb collisions. Notice how a two-temperature structure develops naturally in this model, so that the electrons do not get any hotter than $\text{few} \times 10^{10}$ K. As already discussed in §4, this is the kind of electron temperature needed to fit the spectral data. The brightness temperature of Sgr A* at mm wavelengths is also measured to be of this order [78].

5.3 The Flare in Sgr A*

The long-dashed curve in Fig. 4 shows the spectrum of a model with $\delta = 1$, with all the viscous heat assumed to go into the electrons. The electrons are hotter in this model than in the other two models. Correspondingly, both the synchrotron peak and the Compton-scattering component are significantly stronger. The bremsstrahlung emission is not affected since it is emitted from large radii, where δ has very little effect on the temperature (Fig. 5).

It is interesting that the model with $\delta = 1$ fits both the X-ray flux and the X-ray spectral slope of the flare state of Sgr A*. Moreover, the spectrum passes through the $2.2 \mu\text{m}$ upper limit. As discussed in §2.1, this limit corresponds to a claimed detection of Sgr A*. Could it be that Sgr A* underwent a flare during that particular observation?

It is certainly a coincidence that the $\delta = 1$ model fits the flare data so well, all the more so since the models are not very reliable in this limit. However, the result does show that any minor perturbation that heats up the electrons at small radii by as little as a factor of 2 will produce a spectrum similar to that seen in the flare. Such a temperature change could be caused by many effects. Apart from an increase in δ , other possibilities are (i) a sudden enhancement in the coupling between ions and electrons, (ii) a major reconnection event, or (iii) a sudden injection of a population of nonthermal electrons.

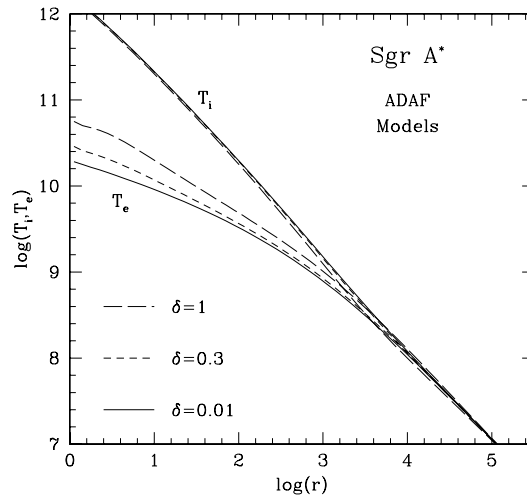


Fig. 5. Variation of the ion and electron temperatures with radius in the three ADAF models shown in Fig. 4

5.4 Does Sgr A* Have an Event Horizon?

Even allowing for the fact that the accretion rate in an ADAF model is smaller than in the Bondi model by a factor $\sim \alpha$, Sgr A* is still highly underluminous: $L_{acc} \ll 0.1 \dot{M}_{ADAF} c^2$. Energy advection is the reason why the radiative efficiency of the accretion flow is so low. But advection alone is not enough, because we still have to decide what happens to the advected energy when it finally reaches the center. In the models shown in Fig. 4, it was assumed that the mass at the center is a BH which swallows the advected energy.

What would happen if the object were not a BH? If the object had a hard surface, then the advected energy would be radiated when the hot gas hit the surface (because the density would go up and the radiative efficiency would increase suddenly), and the predicted spectrum would disagree violently with the data [11],[79]. Figure 6 shows some results. The various curves correspond to ADAF models in which the object in the center is postulated to have a hard surface with radius equal to $10^{0.5}, 10^1, 10^{1.5}, 10^2, 10^{2.5}, 10^3$ Schwarzschild radii. Notice that all the models are ruled out by the infrared limits.

We thus conclude that, if the ADAF model is the correct description of the accretion flow in Sgr A*, then the central object must be a black hole with an event horizon. The same is true even if the accretion proceeds via a Bondi flow.

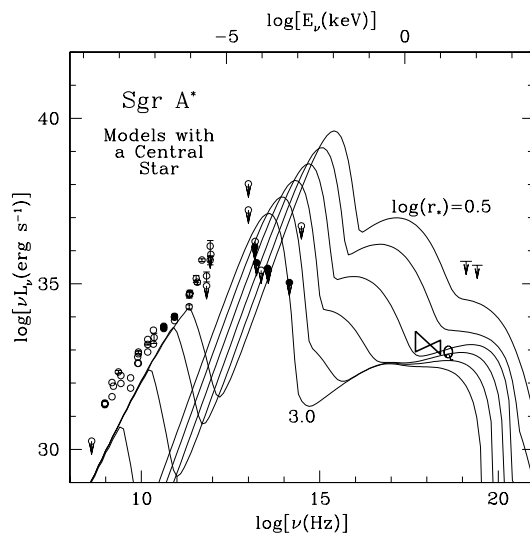


Fig. 6. Spectra of models in which accretion occurs via an ADAF and the central accreting mass is assumed to have a surface that radiates the advected energy with a blackbody spectrum. The curves are labeled by the radius r_* of the central mass in units of the Schwarzschild radius.

6 Other Dim Galactic Nuclei

6.1 Nuclei of Giant Ellipticals

It has long been recognized that the nuclei of nearby giant elliptical galaxies are unusually dim [80], with $L_{acc} \ll 0.1\dot{M}_{Bondi}c^2$. Soon after the successful application of the two-temperature ADAF model to Sgr A* [67], it was proposed that the same model would also solve the riddle of dim elliptical nuclei [81],[82],[83],[84].

Until recently, \dot{M}_{Bondi} in the giant ellipticals was estimated indirectly by modeling the X-ray cooling flow in the central regions of the galaxy and extrapolating the model to the nucleus. However, the Chandra X-ray Observatory has improved matters significantly by providing in a few ellipticals direct images of hot X-ray emitting gas close to the capture radius of the SMBH. Good quality data are presently available for NGC 1399, NGC 4472, NGC 4636 [85] and NGC 6166 [86]. From these observations, reliable estimates of \dot{M}_{Bondi} have been obtained, and we are now in a position to state with great confidence that L_{acc} is indeed very much less than $0.1\dot{M}_{Bondi}c^2$ in all these galactic nuclei.

In fact, L_{acc} is so low and \dot{M}_{Bondi} is so large that even a two-temperature ADAF model with $\dot{M}_{ADAF} = \dot{M}_{Bondi}$ cannot satisfy the X-ray constraints [85]. This is shown for NGC 1399 by the dashed line in Fig. 7. The predicted spectrum is far too bright in X-rays compared to the Chandra upper limit. However, as

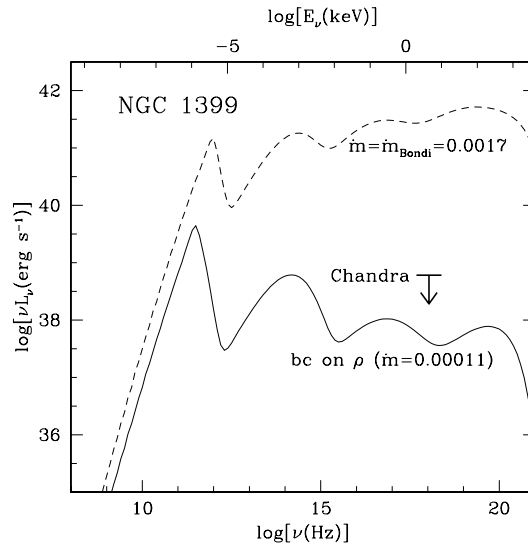


Fig. 7. ADAF models of NGC 1399. For the dashed curve, \dot{M} has been set equal to the estimated Bondi accretion rate (0.0017 in Eddington units). For the solid line, the ADAF model has been adjusted so as to match the external density as measured by Chandra ($\dot{m} = 0.00011$).

explained earlier, it is not correct to set $\dot{M}_{ADAF} = \dot{M}_{Bondi}$. Rather, one must match the density of the ADAF model to the ambient density of the external medium at $R = R_c$ and solve consistently for \dot{M}_{ADAF} . When this is done, one obtains a lower value of \dot{M}_{ADAF} , and correspondingly a significantly dimmer source. The solid line in Fig. 7 shows the spectrum thus obtained for NGC 1399 (using $\alpha = 0.1$, but the results are not very sensitive to this choice). The model is consistent with the X-ray data. Similar results are obtained for other nuclei for which there is Chandra data.

The matching of the ADAF solution to the external medium was done somewhat approximately here. Ideally, one should obtain a consistent solution of the viscous accretion equations, extending from the external medium/cooling flow through the capture radius down to the BH. The analogous problem for spherical accretion has been solved [87], but the viscous problem is yet to be analysed.

6.2 LINERS

Low-Ionization Nuclear Emission Region (LINER) galaxies, and more generally low luminosity AGN (LLAGN), have unusual spectral properties [88]. It has been proposed that the observations could be understood if accretion proceeds via an ADAF in these galactic nuclei [89],[91]. A feature of the proposed models is that the accretion flow consists of two zones: an outer thin disk that extends from some large radius down to a transition radius R_{tr} and an inner ADAF that extends from R_{tr} to the BH horizon.

There is some direct evidence for such a geometry of the accretion flow in NGC 4258 [90], M81 and NGC 4579 [91]. M81 and NGC 4579, in particular, lack the Big Blue Bump that is seen in AGN. Instead, they have a red bump, which can be fitted only with a truncated disk [91]. Furthermore, the absence of short time scale variability [92] and unusually strong radio emission [93] in LLAGN appear to confirm the presence of radiatively inefficient accretion in these galactic nuclei.

6.3 Transition From Thin Disk to ADAF

So far in this article, we have discussed three kinds of accretion flows. First, we briefly mentioned bright AGN, with accretion luminosities of say $L_{acc} \sim 0.1 - 1L_{Edd}$. We said that these objects have Shakura-Sunyaev thin accretion disks. Next, at the other extreme, we discussed Sgr A*, with $L_{acc} \sim 10^{-8.5}L_{Edd}$. We said that this source might have an ADAF extending from the capture radius at $R \sim 10^5 R_S$ down to the BH. Finally, in the previous subsection, we discussed intermediate cases like M81, with $L_{acc} \sim 10^{-4} - 10^{-5}L_{Edd}$. We argued that the accretion occurs via a thin disk at large radii ($R > R_{tr} \sim 10^2 R_S$ [91]) and via an ADAF at smaller radii ($R < R_{tr}$).

The pattern suggested by the above facts is very reminiscent of a paradigm that was developed for BH X-ray binaries [94],[56],[95]. The key idea is that the geometry of the accretion flow is determined primarily by the Eddington-scaled mass accretion rate $\dot{m} = \dot{M}/\dot{M}_{Edd}$. For \dot{m} greater than a critical value

$\dot{m}_{crit} \sim 0.01 - 0.1$, the accretion occurs via a radiatively efficient thin disk, with perhaps a hot corona. At these accretion rates, the ADAF solution is not allowed [48] because the gas density is too high to permit a radiatively inefficient flow. Once \dot{m} falls below \dot{m}_{crit} , an ADAF is allowed at small radii and the thin disk develops a small hole in the inner regions where the cold gas switches to a hot ADAF. The range of radius over which an ADAF is allowed increases as \dot{m} decreases [48], and correspondingly the hole in the thin disk also becomes larger. For an extremely low accretion rate, e.g., $\dot{m} \sim 10^{-5}$ in Sgr A*, the hole is so large that the outer thin disk disappears altogether and the accretion occurs via a pure ADAF over a wide range of radius. Such flows are radiatively extremely inefficient. This paradigm is in qualitative agreement with a variety of observations, e.g., [96], though undoubtedly there are parameters other than \dot{m} that also affect the geometry of the flow.

An important question is: how does the cold gas in a thin disk switch to a hot quasi-spherical ADAF? A number of papers have been written on this “evaporation” process [97],[98],[99],[100],[101], [102],[103],[104], and there is some qualitative understanding of the relevant physics. However, there is no reliable quantitative model yet that can calculate the dependence of the transition radius R_{tr} on the accretion rate \dot{m} .

7 Other Possibilities

7.1 Bondi Accretion With Magnetic Fields

Recently, the first three-dimensional numerical simulations of spherical accretion with magnetic fields were reported [105]. The results turned out to be unexpected. The density profile of a magnetized spherical flow was found to differ significantly from the $R^{-3/2}$ behavior predicted by the Bondi model (§4), and the mass accretion rate was found to be much less than the value given in (2). The reason for the discrepancy is as follows [105].

As already noted in §4, when magnetic fields are frozen into the inflowing gas, the fields are amplified, causing them to reconnect, and the energy released thereby heats up the gas. Since the gas radiates very little of its energy, the entropy of the gas increases inward. The negative radial entropy gradient causes the gas to be convectively unstable, so violent convection is set up. Figure 8 shows velocity streamlines in the meridional plane from one of the numerical simulations. Notice how turbulent the flow is, and how different it is from the purely radial streamlines of Bondi’s hydrodynamic model. In this convective flow, the outward energy flux due to convection dominates the physics at large radii. As a result, the global structure of the flow is strongly affected and the mass accretion rate onto the BH is much reduced from the Bondi rate.

An analytical model of spherical accretion with convection has been developed [105]. The model predicts that the density should vary as $\rho \propto R^{-1/2}$ rather than the Bondi scaling of $\rho \propto R^{-3/2}$. The scaling drops out naturally just from the assumption that the convective energy flux dominates over other fluxes. Because of the modified scaling, the accretion rate onto the BH is much reduced

from the Bondi rate (2):

$$\dot{M}_{MHD} \sim (R_S/R_c)\dot{M}_{Bondi}. \quad (6)$$

The numerical simulations do not have sufficient dynamic range, nor have they been run long enough, to unequivocally confirm this result. What is clear from the simulations, however, is that magnetic fields can modify even such a long-cherished paradigm as the Bondi model.

As discussed in §4.2, the Bondi model is unlikely to be relevant for real accretion flows because it ignores the angular momentum of the gas. It might therefore appear that the above results are not of practical importance. However, as we discuss next, convection causes similarly large effects even in rotating viscous flows. (Historically, the rotating flows were studied first.)

7.2 Convection-dominated Accretion Flow (CDAF)

An ADAF has two unusual properties that strongly influence the global structure of the flow.

First, the gas has a positive Bernoulli parameter (sum of potential energy, kinetic energy and enthalpy), which means that the gas is technically not bound to the BH and is liable to flow out of the system [46],[47],[106]. If the outflow is strong enough, then the amount of mass reaching the BH could be a great deal less than the mass supplied on the outside [107],[108] (but see [109],[110]).

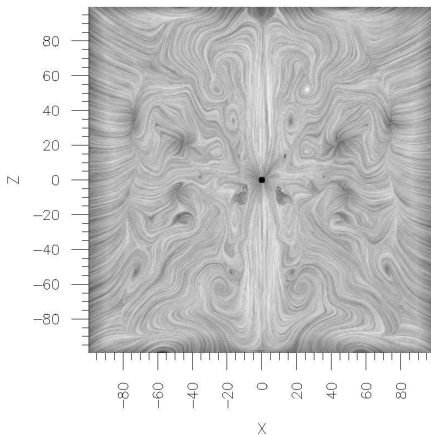


Fig. 8. Velocity streamlines in the meridional plane in a simulation of a magnetized spherical accretion flow [105]. Note the obvious turbulent eddies which are due to convection.

In such an “advection-dominated inflow outflow solution” (ADIOS), the density profile can be strongly modified: instead of $\rho \propto R^{-3/2}$ as in a standard ADAF, one could have $\rho \propto R^{-3/2+p}$, with $0 < p < 1$ [107]. The limit $p = 0$ corresponds to the standard ADAF model described in §5.

Second, because viscous dissipation in an ADAF adds heat energy to the accreting gas, and since there is negligible cooling, the entropy of the gas increases inward (see the analogous discussion in §7.1). As a result, the gas in an ADAF is convectively unstable [111],[46],[47]. The effect of this convection has been studied via numerical hydrodynamic simulations [113],[114],[115],[116]. As in the case of the magnetic Bondi flow, convection alters the density profile to $\rho \propto R^{-1/2}$ and causes the mass accretion rate onto the BH to be reduced drastically compared to the standard ADAF model [115]. The physics of these “convection-dominated accretion flows” (CDAFs) is fairly well understood [117],[118],[119]. Convection introduces a strong flow of energy outward, just as in the magnetized Bondi problem. In addition, it also introduces a flow of angular momentum *inward* (i.e. opposite to the direction of viscous transport), as anticipated in some previous work [120],[121],[122]. All of this leads to novel and quite interesting properties [117],[118]. Analysis of the global structure of CDAFs indicates that the gas switches from a convection-dominated state to a more traditional ADAF-like state for radii less than about $50R_S$ [123].

Preliminary work has been done on the effect of magnetic fields on rotating advection-dominated flows [124],[125],[126],[127],[128],[129]. Depending on the initial configuration of the magnetic field, the dynamical properties of the flow appear to be quite distinct. For a predominantly “vertical” initial field, there are strong jets [124], whereas for a toroidal initial field there are only weak outflows [126]. Regardless, convection seems to be present in both cases, and some studies [128] find quite good agreement between numerical MHD simulations and analytical work on hydrodynamical CDAFs. Others, however, claim that there are large differences (see especially [130] where it is argued that convection in a differentially rotating magnetized medium behaves very differently from the unmagnetized case).

Work in this area is very important and needs to be pursued vigorously. The reason is that pure hydrodynamical simulations are ultimately limited by the fact that they invoke an artificial viscosity (parameterised via α) to transport angular momentum. If the shear stress is generated by the magneto-rotational instability [40], as universally believed, then it is obviously much better to carry out full MHD simulations so that the magnetic shear stress and the associated “viscosity” are computed self-consistently.

The variability properties of MHD flows have been investigated [131],[132]. It is clear that magnetic flares associated with reconnection events occurring over a wide range of scales can give broad-band fluctuations as well as occasional strong outbursts (as in the Sgr A* flare).

7.3 ADIOS/CDAF Models of Sgr A*

Spectral calculations with the ADIOS model using different values of the parameter p (which measures the strength of the outflow) are described in [112]. The results are as follows. Consider a sequence of models in which p is varied while keeping the density at the outer boundary and all other model parameters fixed. With increasing p , the density and the temperature of the gas near the BH decrease. This causes the synchrotron emission and the Compton emission to drop, without affecting the bremsstrahlung emission (which comes from the outside). The good agreement between the ADAF model and the data in Fig. 4 would then be lost. However, if the parameter p as well as the electron heating parameter δ (§5.1) are both increased simultaneously, then one can recover a good fit with the observations [112]. According to Fig. 4, a standard ADAF model ($p = 0$) with $\delta \sim 0.3$ gives a good fit to the data. By increasing p and δ simultaneously, larger values of p are also likely to give acceptable results.

Although the CDAF model has very different physics than the ADIOS model, nevertheless, as far as spectral calculations are concerned, it behaves very much like an ADIOS model with $p = 1$. Spectra corresponding to CDAF models have been presented in the literature [133], but no results are available specifically for Sgr A*. It is possible that even with $\delta = 1$, i.e. with all the viscous energy going into the electrons, the spectrum may still be deficient in the radio/mm band relative to the data. The X-ray spectrum might also be a little too soft. These are not necessarily bad, but they imply that one would need to include additional components in the model, or additional physics, to explain the observations. In the former category would be jet models such as those described below, and in the latter category would be models that include nonthermal electrons.

Although the theoretical motivations behind the ADIOS and CDAF models are strong, there is as yet no unambiguous observational evidence for these models in astrophysical sources. If a claimed detection [134] of linear polarization of Sgr A* in mm waves is confirmed (but see [138]), it would strongly suggest that the density of gas close to the BH is much less than that predicted by the ADAF model [135],[136]. An ADIOS model with a largish value of p or a CDAF model (which is equivalent to $p = 1$) would then be indicated. The discovery of radio variability with a possible 106 day cycle [137] independently suggests the presence of a turbulent CDAF. However, none of these indications is particularly robust at this time.

7.4 Jets, Other Components

In the discussion so far, it has been tacitly assumed that the accretion flow is the source of all the observed radiation. In bright AGN, it is known that radio emission is usually associated with relativistic jets. Since Sgr A* is brightest in radio and mm waves, it is not unreasonable to suppose that some of the observed radiation at these wavelengths originates in a jet, or some other component that is external to the accretion flow. Models of this kind have been developed by several groups (see [12] for a review).

In the context of jet models, we note that a pure accretion model with an ADAF does a pretty good job of explaining the data on Sgr A* (Fig. 4). As explained in §5.2, the model has almost no free parameters, since the accretion rate is fixed by the Chandra observations. If Sgr A* does have an ADAF, then there is very little room for additional emission from a jet.

On the other hand, if the accretion flow corresponds to an ADIOS or a CDAF, then the accretion flow might produce very little radio or mm emission, especially if δ is small. In this case, almost all the radio and mm emission could be from something other than the accretion flow. Jet models then become attractive (but see [140]).

Note that most of the quiescent X-ray emission in Sgr A* is spatially resolved [13]. Therefore, jet models of the quiescent emission need to ensure that they do not predict too much emission in X-rays, since the jet emission is expected to be unresolved. During the X-ray flare in Sgr A*, all the observed excess emission was point-like and so this emission could in principle be entirely from a jet.

Successful disk-plus-jet models have been developed for Sgr A* in which synchro-Compton emission from a compact nozzle region of a jet produces the observed radiation [141],[142],[143],[144]. The “disk” in these models is unlikely to be a standard thin disk for the reasons discussed in §3. Indeed, recent work suggests that a jet-plus-ADAF model is able to combine many of the attractive features of both models [140]. A jet also provides a convincing explanation for the flare in Sgr A* [145].

One interesting result is that the electron energy distribution in Sgr A* has to be nearly mono-energetic in order to fit the sharp cutoff of the spectrum in the infrared [146],[147]. This is a somewhat curious result, since jets in bright AGN almost always have power-law energy distributions. If the relativistic electrons in jets are accelerated via shocks, there must be something very different about the shock in very low-luminosity systems like Sgr A*.

8 Summary and Conclusions

The Chandra X-ray Observatory has eliminated a major uncertainty that has hampered our understanding of dim galactic nuclei. Thanks to Chandra’s excellent angular resolution, we now have direct measurements of the density and temperature of ambient gas close to the gravitational capture radius of the SMBHs in Sgr A* and a few nearby galactic nuclei. This information allows us to estimate for these nuclei the Bondi mass accretion rate \dot{M}_{Bondi} , as well as the accretion rate in an advection-dominated accretion flow \dot{M}_{ADAF} . With the uncertainty in \dot{M} removed, we are now in a position to answer the question posed in the title of this article. The answer consists of three parts:

- In all the dim galactic nuclei for which Chandra has provided a direct estimate of \dot{M}_{Bondi} , the accretion rate is found to be well below the Eddington rate. This is in contrast to bright AGN which are believed to accrete at close to the Eddington rate. Thus, the first, and obvious, reason why AGN switch

off is that the gas supply to the SMBH is reduced, presumably because most of the gas has been converted into stars.

- Even after allowing for the reduced \dot{M} , the objects studied are still anomalously dim: $L_{acc} \ll 0.1\dot{M}_{Bondi}c^2$. Therefore, we can state with great confidence that the accretion *must* proceed via a radiatively inefficient mode. A two-temperature ADAF model fits the available data quite well (Fig. 4), with almost no adjustable parameters (only δ needs to be adjusted, and even it is loosely constrained: §5.2). In this model, there is not much room for additional emission from a jet. A Bondi model can also be made to fit the data, provided the accreting gas is taken to be two-temperature (§4.2). However, the neglect of angular momentum of the gas is a serious weakness of the model. Both the ADAF and Bondi models work only if the central object has an event horizon (§5.4). Independently of these results, one can state with high confidence that there is no Shakura-Sunyaev thin disk in Sgr A* (§3).
- Outflows and convection may be important, in which case the mass accretion rate onto the BH may be significantly less than the mass supply on the outside, i.e. $\dot{M}_{BH} \ll \dot{M}_{Bondi}, \dot{M}_{ADAF}$ (see the discussion of ADIOS/CDAF models in §§7.1–7.3). There is as yet no compelling observational evidence for these models, but there are strong theoretical reasons for favoring them. If the accretion flows in Sgr A* and other dim nuclei are of the ADIOS or CDAF type, then the accretion flow may be very dim in radio/mm, and the observed emission in these bands may come from a relativistic jet or some other component external to the accretion flow.

Thus, it appears that three different effects all conspire to make nearby galactic nuclei extraordinarily dim: there is less gas available, the gas accretes via a radiatively inefficient mode, and (perhaps) less gas reaches the BH than is available for accretion.

Acknowledgements: The author thanks Shin Mineshige and Eliot Quataert for useful comments on the manuscript and the W.M. Keck Foundation for support as a Keck Visiting Professor at the Institute for Advanced Study, Princeton. This research was supported by NSF grant AST-9820686.

References

1. J.H. Krolik: *Active Galactic Nuclei* (Princeton University Press, Princeton 1999)
2. N.I. Shakura, S.A. Sunyaev: *A&A*, 24, 337 (1973)
3. I.D. Novikov, K.S. Thorne: in *Blackholes*, ed. by C. DeWitt, B. DeWitt (Gordon & Breach, 1973) p343
4. J.E. Pringle: *ARAA*, 19, 137 (1981)
5. J. Frank, A. King, D. Raine: *Accretion Power in Astrophysics* (Cambridge Univ. Press, Cambridge 1992)
6. A. Koratkar, O. Blaes: *PASP*, 111, 1 (1999)
7. F. Haardt, L. Maraschi: *ApJ*, 380, L51 (1991)

8. F. Haardt, L. Maraschi: ApJ, 413, 507 (1993)
9. D. Richstone et al.: Nature, 395A, 14 (1998)
10. P.G. Mezger, W.J. Duschl, R. Zylka: A&A Rev., 7, 289 (1996)
11. R. Narayan, R. Mahadevan, J.E. Grindlay, R.G. Popham, C. Gammie: ApJ, 492, 554 (1998)
12. F. Melia, H. Falcke: ARAA, 39, 309 (2001)
13. F.K. Baganoff et al.: ApJ, in press (2001) (astro-ph/0102151)
14. F.K. Baganoff et al.: Nature, 413, 45 (2001)
15. R. Genzel, A. Eckart, T. Ott, F. Eisenhauer: MNRAS, 291, 219 (1997)
16. M.G. Watson, R. Willingale, J.E. Grindlay, P. Hertz: ApJ, 250, 142 (1981)
17. A. Goldwurm et al.: Nature, 371, 589 (1994)
18. P. Predehl, J. Trumper: A&A, 290, L29 (1994)
19. K. Koyama et al.: PASJ, 48, 249 (1996)
20. M. Morris, E. Serabyn: ARAA, 34, 645 (1996)
21. A. Eckart, R. Genzel: MNRAS, 284, 576 (1997)
22. A.M. Ghez, B.L. Klein, M. Morris, E.E. Becklin: ApJ, 509, 678 (1998)
23. R. Genzel, C. Pichon, A. Eckart, O.E. Gerhard, T. Ott: MNRAS, 317, 348 (2000)
24. A.M. Ghez, M. Morris, E.E. Becklin, A. Tanner, T. Kremenek: Nature, 407, 349 (2000)
25. H. Bondi: MNRAS, 112, 195 (1952)
26. S.L. Shapiro, S.A. Teukolsky: *Black Holes, White Dwarfs, and Neutron Stars* (Wiley Interscience, New York, 1983)
27. R.F. Coker, F. Melia: ApJ, 488, L149 (1997)
28. E. Quataert, R. Narayan, M.J. Reid: ApJ, 517, 101 (1999)
29. H. Falcke, F. Melia: ApJ, 479, 740 (1997)
30. V.F. Shvartsman: Sov. Astr., 15, 37 (1971)
31. P. Meszaros: A&A, 44, 59 (1975)
32. F. Melia: ApJ, 387, L25 (1992)
33. F. Melia: ApJ, 426, 577 (1994)
34. R. Mahadevan, R. Narayan, I. Yi: ApJ, 465, 327 (1996)
35. V. Kowalenko, F. Melia: MNRAS, 310, 1053
36. A. Lazarian, E.T. Vishniac: ApJ, 511, 193 (1999)
37. A. Lazarian, E.T. Vishniac: ApJ, 517, 700 (1999)
38. S.L. Shapiro, E.E. Salpeter: ApJ, 198, 671 (1975)
39. S.L. Shapiro, A.P. Lightman, D.M. Eardley: ApJ, 204, 187 (1976)
40. S.A. Balbus, J.F. Hawley: Rev. Mod. Phys., 70, 1 (1998)
41. F. Melia, S. Liu, R. Coker: ApJ, 545, L117 (2000)
42. J.E. Pringle: MNRAS, 178, 195 (1977)
43. R. Popham, R. Narayan: ApJ, 394, 255 (1992)
44. S. Ichimaru: ApJ, 214, 840 (1977)
45. M.J. Rees, M.C. Begelman, R.D. Blandford, E.S. Phinney: Nature, 295, 17 (1982)
46. R. Narayan, I. Yi: ApJ, 428, L13 (1994)
47. R. Narayan, I. Yi: ApJ, 444, 231 (1995)
48. R. Narayan, I. Yi: ApJ, 452, 710 (1995)
49. M. Abramowicz, X. Chen, S. Kato, J.P. Lasota, O. Regev: ApJ, 438, L37 (1995)
50. X. Chen, M.A. Abramowicz, J.P. Lasota, R. Narayan, I. Yi: ApJ, 443, L61 (1995)
51. D. Tsiklauri: New Astron., 6, 487 (2001)
52. R. Mahadevan, E. Quataert: ApJ, 490, 605 (1997)
53. R. Mahadevan, R. Narayan, J. Krolik: ApJ, 486, 268 (1997)
54. R. Mahadevan: MNRAS, 304, 501 (1999)

55. F. Ozel, D. Psaltis, R. Narayan: ApJ, 541, 234 (2000)
56. A.A. Esin, J.E. McClintock, R. Narayan: ApJ, 489, 865; 500, 523 (1997)
57. F. Yuan, Q. Peng, J. Lu, J. Wang: ApJ, 537, 236 (2000) ???
58. T. Piran: ApJ, 221, 652 (1978)
59. S. Kato, M.A. Abramowicz, X. Chen: PASJ, 48, 67 (1996)
60. S. Kato, T. Yamasaki, M.A. Abramowicz, X. Chen: PASJ, 49, 221 (1997)
61. X. Wu, Q. Li: ApJ, 469, 776 (1996)
62. X. Wu: MNRAS, 292, 113 (1997)
63. R. Narayan, R. Mahadevan, E. Quataert: in *The Theory of Black Hole Accretion Discs*, ed. by M.A. Abramowicz, G. Bjornsson, J.E. Pringle (Cambridge Univ. Press, Cambridge, 1998) p148
64. S. Kato, J. Fukue, S. Mineshige: *Black Hole Accretion Disks* (Kyoto Univ. Press, Kyoto, 1998)
65. E. Quataert: in *Probing the Physics of Active Galactic Nuclei by Multiwavelength Monitoring*, ed. by B.M. Peterson, R.S. Polidan, R.W. Pogge (Astr. Soc. Pacific, San Francisco, 2001) p71
66. R. Narayan, M.R. Garcia, J.E. McClintock: in *Proc. IX Marcel Grossmann Conference*, in press (2001) (astro-ph/0107387)
67. R. Narayan, I. Yi, R. Mahadevan: Nature, 374, 623 (1995)
68. T. Manmoto, S. Mineshige, M. Kusunose: ApJ, 489, 791 (1997)
69. R. Mahadevan: Nature, 394, 651 (1998)
70. T. Manmoto: ApJ, 534, 734 (2000)
71. E.S. Phinney: in *Plasma Astrophysics*, ed. by T. Guyenne (ESA SP-161, 1981) p337
72. G.S. Bisnovatyi-Kogan, R.V.E Lovelace: ApJ, 486, L43 (1997)
73. E. Quataert: ApJ, 500, 978 (1998)
74. A. Gruzinov: ApJ, 501, 787 (1998)
75. E. Quataert, A. Gruzinov: ApJ, 520, 248 (1999)
76. E. Blackman: MNRAS, 302, 723 (1999)
77. K.E. Nakamura, M. Kusunose, R. Matsumoto, S. Kato: PASJ, 49, 503 (1997)
78. S.S. Doeleman et al.: AJ, 121, 2610 (2001)
79. K. Menou, E. Quataert, R. Narayan: in *Black Holes, Gravitational Radiation and the Universe*, ed. by B.R. Iyer, B. Bhawal (Kluwer, Dordrecht, 1999) p265
80. A.C. Fabian, C.R. Canizares: Nature, 333, 829 (1988)
81. A.C. Fabian, M.J. Rees: MNRAS, 277, L5 (1995)
82. C.S. Reynolds, T. di Matteo, A.C. Fabian, U. Hwag, C.R. Canizares: MNRAS, 283, L111 (1996)
83. R. Mahadevan: ApJ, 477, 585 (1997)
84. T. di Matteo, A.C. Fabian: MNRAS, 286, 50 (1997)
85. M. Loewenstein, R.F. Mushotzky, L. Agnelini, K.A. Arnaud, E. Quataert: ApJ, 555, L21 (2001)
86. T. di Matteo, R.M. Johnstone, A.C. Fabian, S.W. Allen: ApJ, 550, L19 (2001)
87. E. Quataert, R. Narayan: ApJ, 528, 236 (2000)
88. L.C. Ho: ApJ, 516, 672 (1999)
89. J.P. Lasota, M.A. Abramowicz, X. Chen, J. Krolik, R. Narayan, I. Yi: ApJ, 462, 142 (1996)
90. C.F. Gammie, R. Narayan, R. Blandford: ApJ, 516, 177 (1999)
91. E. Quataert, T. di Matteo, R. Narayan, L.C. Ho: ApJ, 525, L89 (1999)
92. A. Ptak, T. Yaqoob, R. Mushotzky, P. Serlemitsos, R. Griffiths: ApJ, 501, L37 (1998)

93. J.S. Ulvestad, L.C. Ho: ApJ, 562, L133 (2001)
94. R. Narayan: ApJ, 461, 136 (1996)
95. A.A. Esin, R. Narayan, W. Cui, J.E. Grove, S.N. Zhang: ApJ, 505, 854 (1998)
96. A.A. Esin, J.E. McClintock, J.J. Drake, M.R. Garcia, C.A. Haswell, R.I. Hynes, M.P. Muno: ApJ, 555, 483 (2001)
97. F. Meyer, E. Meyer-Hofmeister: A&A, 361, 175 (1994)
98. F. Honma: PASJ, 48, 77 (1996)
99. C.P. Dullemond, R. Turolla: ApJ, 503, 361 (1998)
100. B.F. Liu, W. Yuan, F. Meyer, E. Meyer-Hofmeister, G.Z. Xie: ApJ, 527, L17 (1999)
101. A. Rozanska, B. Czerny: A&A, 360, 1170 (2000)
102. B. Czerny, A. Rozanska, P.Y. Zycki: New Astron. Rev., 44, 439 (2000)
103. F. Meyer, B.F. Liu, E. Meyer-Hofmeister: A&A, 361, 175 (2000)
104. H.C. Spruit, B. Deufel: A&A, submitted (2001) (astro-ph/0108497)
105. I.V. Igumenshchev, R. Narayan: ApJ, in press (2001) (astro-ph/0105365)
106. R. Narayan, S. Kato, F. Honma: ApJ, 476, 49 (1997)
107. R.D. Blandford, M.C. Begelman: MNRAS, 303, L1 (1999)
108. T. Beckert: ApJ, 539, 223 (2000)
109. M.A. Abramowicz, J.P. Lasota, I.V. Igumenshchev: MNRAS, 314, 775 (2000)
110. R. Turolla, C.P. Dullemond: ApJ, 531, L49 (2000)
111. M.C. Begelman, D.L. Meier: ApJ, 253, 873 (1982)
112. E. Quataert, R. Narayan: ApJ, 520, 298 (1999)
113. I.V. Igumenshchev, X. Chen, M.A. Abramowicz: MNRAS, 278, 236 (1996)
114. I.V. Igumenshchev, M.A. Abramowicz: MNRAS, 303, 309 (1999)
115. J.M. Stone, J.E. Pringle, M.C. Begelman: MNRAS, 310, 1002 (1999)
116. I.V. Igumenshchev, M.A. Abramowicz: ApJ, 537, L27 (2000)
117. R. Narayan, I.V. Igumenshchev, M.A. Abramowicz: ApJ, 539, 798 (2000)
118. E. Quataert, A. Gruzinov: ApJ, 539, 809 (2000)
119. I.V. Igumenshchev, M.A. Abramowicz, R. Narayan: ApJ, 537, L27 (2000)
120. D. Ryu, J. Goodman: ApJ, 388, 438 (1992)
121. P. Kumar, R. Narayan, A. Loeb: ApJ, 453, 480 (1995)
122. J.M. Stone, S.A. Balbus: ApJ, 464, 364 (1996)
123. M.A. Abramowicz, I.V. Igumenshchev, E. Quataert, R. Narayan: ApJ, in press (2001) (astro-ph/0110371)
124. R. Matsumoto: in *Numerical Astrophysics*, ed. by S.M. Miyama, K. Tomisaka, T. Hanawa (Kluwer, Dordrecht, 1999), p195
125. J.F. Hawley: ApJ, 528, 462 (2000)
126. M. Machida, M.R. Hayashi, R. Matsumoto: ApJ, 532, L67 (2000)
127. J.M. Stone, J.E. Pringle: MNRAS, 322, 461 (2001)
128. M. Machida, R. Matsumoto, S. Mineshige: PASJ, 53, L1 (2001)
129. J.F. Hawley, S.A. Balbus, J.M. Stone: ApJ, 554, L49 (2001)
130. S.A. Balbus: ApJ, 562, 909 (2001)
131. T. Kawaguchi, S. Mineshige, M. Machida, R. Matsumoto, K. Shibata: PASJ, 52, L1 (2000)
132. S. Mineshige, H. Negoro, R. Matsumoto, M. Machida: this volume (2001)
133. G.H. Ball, R. Narayan, E. Quataert: ApJ, 552, 221 (2001)
134. D.K. Aitken et al.: ApJ, 534, L173 (2000)
135. E. Quataert, A. Gruzinov: ApJ, 545, 842 (2000)
136. E. Agol: ApJ, 538, L121 (2000)
137. J.H. Zhao, G.C. Bower, W.M. Goss: ApJ, 547, L29 (2001)

138. G.C. Bower, M.C.H. Wright, H. Falcke, D.C. Backer: ApJ, 555, L103 (2001)
139. H. Falcke: in *Reviews in Modern Astronomy 14: Dynamical Stability and Instabilities in the Universe*, ed. by R.E. Schielicke (Astronomische Gesellschaft, Hamburg, 2001) p15
140. F. Yuan, S. Markoff, H. Falcke: A&A, in press (2001) (astro-ph/0112464)
141. H. Falcke, K. Mannheim, P.L. Biermann: A&A, 278, 71 (1993)
142. H. Falcke: in *IAU Symp. 169: Unsolved Problems in the Milky Way*, ed. by L. Blitz, P.J. Teuben (Kluwer, Dordrecht, 1996) p163
143. H. Falcke, P.L. Biermann: A&A, 342, 49 (1999)
144. H. Falcke, S. Markoff: A&A, 362, 113 (2000)
145. S. Markoff, H. Falcke, F. Yuan, P.L. Biermann: A&A, 379, L13 (2001)
146. W.J. Duschl, H. Lesch: A&A, 286, 431 (1994)
147. T. Beckert, W.J. Duschl: A&A, 328, 95 (1997)